# Global QBO in Circulation and Ozone. Part II: A Simple Mechanistic Model

K. K. TUNG AND H. YANG

*Department of Applied Mathematics, University of Washington, Seattle, Washington*

(Manuscript received 6 August 1993, in final form 18 February 1994)

ABSTRACT

Although the phenomenon of *equatorial* quasi-biennial oscillation is relatively well understood, the problem of how the equatorially confined QBO wave forcing can induce a signal in the extratropics of comparable or larger magnitude remains unsolved. A simple mechanistic model is constructed to provide a quantitative test of the hypothesis that the phenomenon of extratropical QBO is mainly caused by an anomalous seasonal circulation induced by an anomalous Eliassen–Palm flux divergence. The anomaly in E–P flux divergence may be caused in turn by the relative poleward and downward shift of the region of irreversible mixing (breaking) of the extratropical planetary waves during the easterly phase of the equatorial QBO as compared to its westerly phase. The hemispheric nature of the anomaly wave forcing in solstice seasons (viz., no wave breaking in the summer hemisphere) induces a global circulation anomaly that projects predominantly into the first few zonal Hough modes of Plumb. Such a global QBO circulation pattern, although difficult to measure directly, is reflected in the distribution of stratospheric tracers transported by it. Our model produces a global pattern of QBO anomaly in column ozone that appears to account for much of the unfiltered interannual variability in the column ozone observed by the TOMS instrument aboard the Nimbus satellite. Furthermore, the model produces the characteristic spectrum of the observation with peaks at periods of 20 and 30 months.

## 1. Introduction

There has been some controversy concerning whether or not the extratropical quasi-biennial oscillation (QBO) phenomenon involves an anomaly in the mean meridional transport circulation (see Part I for references and discussion). Current measurement and data analysis techniques are not adequate to directly detect on a global basis such a circulation, if one exists. One can, nevertheless, infer its existence from the behavior of tracers transported by it. For example, ozone, being a tracer in the lower stratosphere, seems to exhibit a very significant QBO component in its interannual variability in both Tropics and extratropics.

As pointed out in Part I, the observed column ozone interannual variability in the extratropics contains at most 20%–30% [6–8 Dobson units (DU)] that is in the frequency range of equatorial QBO. A significant portion of the remaining anomaly is in the 20-month period, which can be thought of as the modulation of a seasonal anomaly (with a 12-mo period) by the 30-month QBO period. We argue that the extratropical QBO phenomenon in ozone cannot be satisfactorily explained with respect to either the magnitude or the seasonal synchronization in the observed data without the presence of a seasonal QBO anomaly in the transport circulation. In contrast, Gray and Pyle (1989), Chipperfield and Gray (1992), and recently Gray and Ruth (1993) claimed to have simulated extratropical QBO in column ozone with seasonal synchronization using a 2D model with fixed (i.e., no interannual variability) extratropical advective and diffusive transports.

Observational studies of the dynamical QBO phenomenon in the extratropics seem to favor the presence of a QBO component in the transporting circulation forced by a QBO anomaly in the Eliassen–Palm (E–P) flux divergence (see Part I for references). The body of observational evidence, when taken together, suggests an oscillation dynamically consistent among the various dynamical quantities and the transport of long-lived tracers.

We propose the following dynamical framework as an aid to understanding the reported oscillations in various quantities. It is similar to the one originally proposed by Holton and Tan (1980), with the modification that allows the mechanism to become less dependent on the delicate role played by the zero-wind line. More importantly, it provides a way to generate a QBO anomaly in the extratropical circulation significantly poleward of the zero-wind line. Instead of viewing the atmospheric wave–mean flow system as quasi-linear or weakly nonlinear, one should perhaps treat it as fully nonlinear and near saturation near the 10-mb level and above. Because of the exponential decrease in density with height, a planetary-scale stationary wave forced near the earth's surface propagates to the stratosphere generally with amplitude increase. At some level its amplitude would become large enough for it to "break," resulting in a cascade of energy and entropy

*Corresponding author address:* Dr. Ka Kit Tung, Department of Applied Mathematics FS-20, University of Washington, Seattle, WA 98195.

# Global QBO in Circulation and Ozone. Part II: A Simple Mechanistic Model

K. K. TUNG AND H. YANG

*Department of Applied Mathematics, University of Washington, Seattle, Washington*

(Manuscript received 6 August 1993, in final form 18 February 1994)

ABSTRACT

Although the phenomenon of *equatorial* quasi-biennial oscillation is relatively well understood, the problem of how the equatorially confined QBO wave forcing can induce a signal in the extratropics of comparable or larger magnitude remains unsolved. A simple mechanistic model is constructed to provide a quantitative test of the hypothesis that the phenomenon of extratropical QBO is mainly caused by an anomalous seasonal circulation induced by an anomalous Eliassen–Palm flux divergence. The anomaly in E–P flux divergence may be caused in turn by the relative poleward and downward shift of the region of irreversible mixing (breaking) of the extratropical planetary waves during the easterly phase of the equatorial QBO as compared to its westerly phase. The hemispheric nature of the anomaly wave forcing in solstice seasons (viz., no wave breaking in the summer hemisphere) induces a global circulation anomaly that projects predominantly into the first few zonal Hough modes of Plumb. Such a global QBO circulation pattern, although difficult to measure directly, is reflected in the distribution of stratospheric tracers transported by it. Our model produces a global pattern of QBO anomaly in column ozone that appears to account for much of the unfiltered interannual variability in the column ozone observed by the TOMS instrument aboard the Nimbus satellite. Furthermore, the model produces the characteristic spectrum of the observation with peaks at periods of 20 and 30 months.

## 1. Introduction

There has been some controversy concerning whether or not the extratropical quasi-biennial oscillation (QBO) phenomenon involves an anomaly in the mean meridional transport circulation (see Part I for references and discussion). Current measurement and data analysis techniques are not adequate to directly detect on a global basis such a circulation, if one exists. One can, nevertheless, infer its existence from the behavior of tracers transported by it. For example, ozone, being a tracer in the lower stratosphere, seems to exhibit a very significant QBO component in its interannual variability in both Tropics and extratropics.

As pointed out in Part I, the observed column ozone interannual variability in the extratropics contains at most 20%–30% [6–8 Dobson units (DU)] that is in the frequency range of equatorial QBO. A significant portion of the remaining anomaly is in the 20-month period, which can be thought of as the modulation of a seasonal anomaly (with a 12-mo period) by the 30-month QBO period. We argue that the extratropical QBO phenomenon in ozone cannot be satisfactorily explained with respect to either the magnitude or the seasonal synchronization in the observed data without the presence of a seasonal QBO anomaly in the transport circulation. In contrast, Gray and Pyle (1989), Chipperfield and Gray (1992), and recently Gray and Ruth (1993) claimed to have simulated extratropical QBO in column ozone with seasonal synchronization using a 2D model with fixed (i.e., no interannual variability) extratropical advective and diffusive transports.

Observational studies of the dynamical QBO phenomenon in the extratropics seem to favor the presence of a QBO component in the transporting circulation forced by a QBO anomaly in the Eliassen–Palm (E–P) flux divergence (see Part I for references). The body of observational evidence, when taken together, suggests an oscillation dynamically consistent among the various dynamical quantities and the transport of long-lived tracers.

We propose the following dynamical framework as an aid to understanding the reported oscillations in various quantities. It is similar to the one originally proposed by Holton and Tan (1980), with the modification that allows the mechanism to become less dependent on the delicate role played by the zero-wind line. More importantly, it provides a way to generate a QBO anomaly in the extratropical circulation significantly poleward of the zero-wind line. Instead of viewing the atmospheric wave–mean flow system as quasi-linear or weakly nonlinear, one should perhaps treat it as fully nonlinear and near saturation near the 10-mb level and above. Because of the exponential decrease in density with height, a planetary-scale stationary wave forced near the earth's surface propagates to the stratosphere generally with amplitude increase. At some level its amplitude would become large enough for it to "break," resulting in a cascade of energy and entropy

*Corresponding author address:* Dr. Ka Kit Tung, Department of Applied Mathematics FS-20, University of Washington, Seattle, WA 98195.

to smaller scales and an irreversible mixing of tracers and potential vorticity. Satellite observations of wave breaking and resulting ozone transport (McIntyre and Palmer 1984; Leovy et al. 1985) suggest that such a level is reached in the midstratosphere. It is conceivable that the modulation of the westerly waveguide by the equatorial QBO in zonal wind may affect the location of breaking of the planetary waves in the extratropics. They may, for example, break more poleward and at a lower altitude in the easterly phase, and the opposite may happen in the westerly phase.

We envisage the following dynamical scenario for an easterly phase:

1) Equatorial waves (westerly Kelvin and easterly Rossby–gravity waves) force the equatorial QBO in zonal wind and temperature. The induced secondary QBO circulation is equatorially confined (Plumb and Bell 1982; Plumb 1982, 1984).

2) As easterly zonal wind descends into the equatorial midstratosphere, the polar westerly waveguide in the stratosphere for the extratropical stationary waves is narrowed. The amplitudes of the stationary waves become larger as they are focused more poleward [the so-called Holton and Tan mechanism (Holton and Tan 1980; McIntyre 1982)], possibly producing a larger (positive and negative) wave potential vorticity gradient $q_y'$.

3) Enhanced planetary wave breaking may result as the gradient of the total Ertel's potential vorticity, $q_y = \bar{q}_y + q_y'$, becomes negative in regions more poleward and at a lower altitude. [The instability criterion $q_y < 0$ is used here for breaking, following Garcia (1991).]

4) Irreversible mixing due to the breaking planetary waves leads to an E–P flux divergence anomaly, which in turn induces an anomaly in the mean diabatic meridional circulation. The anomaly circulation is responsible for transporting the ozone to create an anomaly in its column density. The zonal mean jet in the lower stratosphere tends to be decelerated more and, through thermal wind, the mean temperature at high latitudes becomes warmer, in a easterly phase. The opposite is true in a westerly phase: less breaking and weaker diabatic circulation result in a stronger zonal jet and colder polar temperature. Many of these features have indeed been observed.

Holton and Tan (1980) composited monthly mean Northern Hemisphere 50-mb geopotential heights for a 16-year period and found that the zonal mean value at high latitudes is significantly lower during the westerly phase of the equatorial QBO than during the easterly phase for all months composited, implying a colder polar vortex and stronger zonal mean winds. The wintertime circumpolar vortex is often observed to be less perturbed in the westerly phase. There are more major sudden warnings in the easterly phase (Labitzke 1982; Dunkerton et al. 1988).

The QBO signal in the E–P flux divergence is more difficult to extract from observations because it is a more differentiated quantity and is therefore more noisy (see Pawson et al. 1993). Holton and Tan (1982) found only a small difference in the E–P flux divergences between the two phases of the QBO. Recently, however, using 25 years of daily NMC data, Dunkerton and Baldwin (1991) have found that the composite E–P fluxes are more convergent in the midlatitudes in the easterly phase of the equatorial QBO than in the westerly phase. Their finding is consistent with what is required to force an extratropical anomaly in the meridional circulation and other zonal mean dynamical variables. The observed tracer distributions can be used to provide an independent check for both the sense and magnitude of this hypothesized circulation. We will use ozone for this purpose.

## 2. E–P flux divergence and the induced meridional circulation

Let $\bar{\psi}$ be the streamfunction for the zonal mean meridional (residual) circulation $(\bar{v}, \bar{w})$:

$$\rho_0\bar{v} = -\frac{\partial}{\partial z}\rho_0\bar{\psi}$$

$$\rho_0\bar{w} = \frac{1}{a}\frac{\partial}{\partial \mu}[\rho_0\bar{\psi}(1-\mu^2)^{1/2}], \qquad (2.1)$$

where $\mu = \sin(\text{latitude})$ and $z = H\ln(p_{00}/p)$, $\rho_0 = \rho_0(0)e^{-z/H}$; other variables retain their usual meaning as in Tung (1986). Under quasigeostrophic assumption, Plumb (1982) showed that $\bar{\psi}$ satisfies the following elliptic partial differential equation [apart from a typographical error in his Eq. (2.9)]:

$$\frac{\partial}{\partial z}\left[\frac{1}{\rho_0}\frac{\partial}{\partial z}(\rho_0\bar{\psi})\right] + \frac{N^2}{4\Omega^2a^2}\frac{(1-\mu^2)^{1/2}}{\mu^2}\frac{\partial^2}{\partial\mu^2}[\bar{\psi}(1-\mu^2)^{1/2}] = \frac{1}{4\Omega^2a}\frac{(1-\mu^2)^{1/2}}{\mu^2}\frac{\partial}{\partial\mu}Q + \frac{1}{2\Omega\mu}\frac{\partial}{\partial z}F. \qquad (2.2)$$

Here $F$ is the net wave forcing of the zonal mean zonal momentum tendency (in m s$^{-1}$/day) and $Q$ is the net diabatic heating rate (in K/day). Equation (2.2) is now applied to the *anomaly* circulation induced by an *anomaly* in E–P flux divergence due to enhanced (reduced) deposition of easterly planetary wave momentum forcing in easterly (westerly) phase of the equatorial QBO. Let $M$ denote such an anomaly, then (see Garcia 1987)

$$F = M - K_R\bar{u}, \quad Q = -\alpha\bar{T}, \qquad (2.3)$$

where $K_R$ is a Rayleigh damping coefficient. Here $-K_R\bar{u}$ is taken to represent mechanical damping of the zonal mean flow and is a crude parameterization of the effects of other waves (such as breaking gravity waves, turbulence, etc.) not represented by the stationary wave contribution designated as $M$. Newtonian damping of the temperature anomaly is incorporated in $\alpha$. If $K_R/\alpha = 1$, the effects of these two terms cancel. Only $M$ remains on the right-hand side of Eq. (2.2). In the more general case of $K_R/\alpha \neq 1$, Garcia (1987) showed that Eq. (2.2) can be rewritten as

$$\frac{\partial}{\partial z}\left[\frac{1}{\rho_0}\frac{\partial}{\partial z}(\rho_0\bar{\psi})\right] + R\frac{N^2}{4\Omega^2a^2}\frac{(1-\mu^2)^{1/2}}{\mu^2} \times \frac{\partial^2}{\partial\mu^2}[\bar{\psi}(1-\mu^2)^{1/2}] = \frac{1}{2\Omega\mu}\frac{\partial}{\partial z}M, \quad (2.4)$$

where

$$R \equiv \frac{K_R + i\omega}{\alpha + i\omega} \approx \frac{K_R}{\alpha}$$

[Garcia assumed that $(\partial\bar{u}/\partial t)/\bar{u} = i\omega = (\partial\bar{T}/\partial t)/\bar{T}$]. For our present application to the QBO, $\omega \sim 2\pi/2$ yr and should be much smaller than either $K_R$ or $\alpha$, which are of the order of the inverse of a few days to a few tens of days. As it turns out (Garcia 1987) the scale of the circulation response to a localized wave forcing in $M$ depends on the magnitude of the parameter $RN^2H^2/(4\Omega^2a^2)$. When this number is small, the circulation response is local and geostrophic:

$$2\Omega\mu\bar{v} \approx M.$$

When that parameter is large, the circulation pattern can become global even when the forcing $M$ is local.

Following Plumb (1982), the circulation response $\bar{\psi}$ and the wave E–P flux forcing $M$ are both expanded in terms of the function $B_n(\mu)$ as

$$\bar{\psi}(\mu, z) = \sum_{n=1}^{\infty} A_n(z)B_n(\mu)$$

$$M(\mu, z) = \sum_{n=1}^{\infty} M_n(z)\mu B_n(\mu). \quad (2.5)$$

The extra factor of $\mu$ in the expansion of $M$ is necessary because it is $M/\mu$, rather than $M$, that appears in Eq. (2.4). The eigenfunction $B_n(\mu)$ satisfies the eigenvalue equation:

$$\frac{(1-\mu^2)^{1/2}}{\mu^2}\frac{d^2}{d\mu^2}[B_n(1-\mu^2)^{1/2}] - \epsilon_n B_n = 0, \quad (2.6)$$

subject to the boundary conditions $B_n(\pm 1) = 0$. The parameter $\epsilon_n$ is the eigenvalues of the system and is related to the equivalent depth $h_n$ of the Laplace tidal equation by

$$\epsilon_n = 4\Omega^2a^2/gh_n.$$

As Plumb (1982) pointed out, all the eigenvalues are real and negative and the following orthogonality relationship holds:

$$-\epsilon_n\int_{-1}^{1}\mu^2B_n(\mu)B_m^*(\mu)d\mu = \delta_{nm},$$

where superscript star denotes complex conjugate and $\delta_{nm}$ is the Kronecker delta function. Substituting (2.5) into Eq. (2.4), we obtain the following vertical structure equation:

$$\frac{d}{dz}\left[\frac{1}{\rho_0}\frac{d}{dz}\rho_0A_n\right] - \Lambda_n^2A_n = \frac{1}{2\Omega}\frac{d}{dz}M_n, \quad (2.7)$$

where $\Lambda_n^2 = -\epsilon_nRN^2/(4\Omega^2a^2)$. In this study we use $N^2 = 4.0 \times 10^{-4}$ s$^{-2}$, $R = 1$, leading to $\Lambda_n^2 = -4.6 \times 10^{-4}\,\epsilon_n$ km$^{-2}$.

The E–P flux divergence anomaly used is the hemispheric form in Garcia (1987). [Note that, strictly speaking, this form does not conserve mass because the E–P flux "divergence" is now not in a divergence form. However, this does not matter since only its derivative is used in the streamfunction equation (2.2)]:

$$M = \begin{cases} 0 & \text{for } \mu \leq 0 \\ -1.5 \times 10^{-5}\,(2\mu(1-\mu^2)^{1/2}) \\ \quad \times \exp[-(z/12\text{ km} - 3)^2]\text{ m s}^{-2} \\ & \text{for } \mu > 0. \end{cases} \quad (2.8)$$

Here $M$ is crudely fitted so that its amplitude in lower to upper stratosphere for the easterly or westerly phase used is half that found by Dunkerton and Balwin (1991) for the easterly minus westerly anomaly. Note that the E–P flux anomaly has a much larger amplitude (more wave breaking) in upper stratosphere than in the lower stratosphere as in the observational data. Therefore, the anomaly circulation that is needed to create an anomaly in column ozone in our model is not driven by wave breaking in the lower stratosphere, as one would probably first expect. It is instead a downward extension of a response to wave breaking anomaly higher up. Dunkerton and Balwin's data show no coherent signal in the lower stratosphere, but a clear dipole anomaly at the 10-mb level and above. In Fig. 1, the induced circulation in the meridional plane is shown. It depicts, in most of stratosphere, a broad feature of a global circulation with downward motion poleward of the northern midlatitudes and gentler upward motion over the rest of the global pattern, extending to the Southern Hemisphere.

The global pattern of zonal mean temperature anomaly is shown in Fig. 2. As pointed out by Randel (1993), this global pattern of temperature anomaly is quite characteristic of the observed large-scale transient events in the stratosphere.

In the equatorial region, the standard theory for the forcing of zonal wind QBO by Kelvin and mixed Rossby–gravity waves is adopted. The same parameters for the amplitudes and phase speeds as adopted by

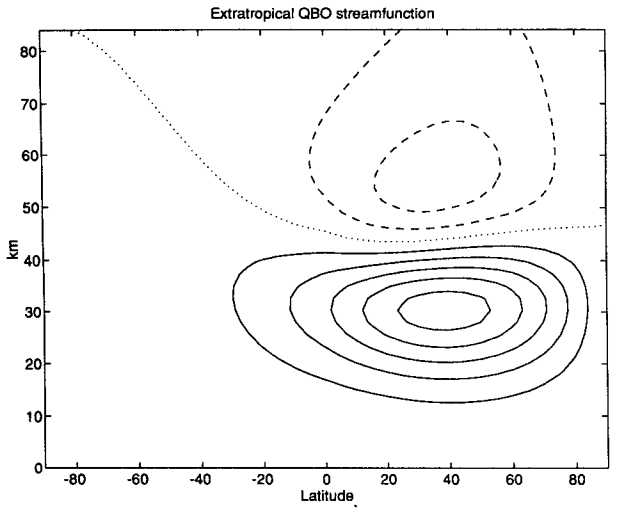


FIG. 1. Extratropical circulation anomaly streamfunction as a response to E–P flux divergence anomaly given in (2.8). Contour levels are 0 (dotted line), ±0.1, ±0.2, . . . $m^2 s^{-1}$, with solid (dashed) lines for positive (negative) contours.

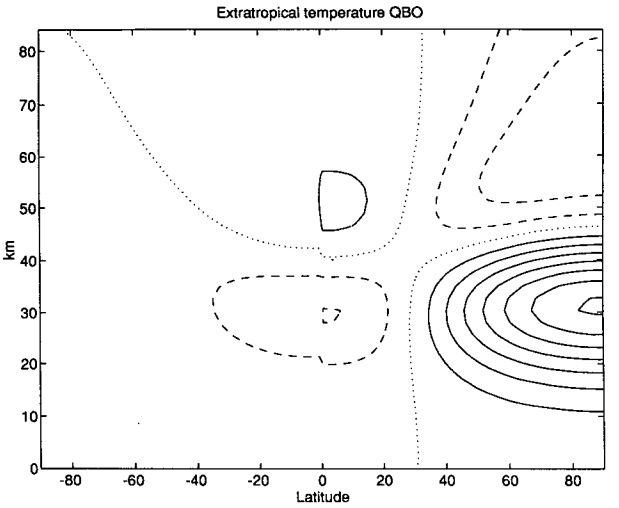


FIG. 2. Zonal mean temperature anomaly corresponding to the circulation anomaly in Fig. 1. Contour levels are 0 (dotted line), ±0.5 K, ±1 K, . . . , with solid (dashed) lines for positive (negative) contours.

Gray and Pyle (1989) are used here, except that for simplicity the same Gaussian width (10 degrees of latitude) for the meridional extent is used for both wave modes (while according to some WKB expressions, the Kelvin wave mode should be wider than the mixed Rossby–gravity modes: 13 deg vs 6.5 deg). The same WKB expression for the E–P flux divergence caused by the absorption of these waves is adopted here. Figure 3 shows a typical circulation pattern during an easterly phase. It shows the typical symmetric QBO secondary circulation with rising motion in the lower stratosphere above the equator and sinking poleward of ±10 degrees in the subtropics. The reverse circulation in the upper stratosphere is not important as far as its effect on the column ozone is concerned.

## 3. Seasonal and interannual variations of circulation anomaly

An E–P flux divergence anomaly results in the westerly wind region from an enhanced or diminished breaking of stationary planetary waves, which do not propagate through an easterly region into the stratosphere. Therefore, it is physically reasonable to assume that the E–P flux divergence anomaly occurs only in the westerly part of the stratosphere, which excludes the summer hemisphere. Thus, a simple seasonal cycle for $M$, the E–P flux divergence anomaly, can be constructed as follows.

For the northern winter season, the hemispheric distribution of (2.8) is used in which the Southern Hemisphere has no E–P flux anomaly. For the northern summer, which is the southern winter, the North and South Poles in (2.8) are switched. The $M$ for the equinox seasons is set to be zero. A simple periodic function in time is fitted to these four points to form a complete seasonal cycle.

To describe the year to year variations, the circulation anomaly is multiplied by a "QBO index," chosen to have a positive sign during the easterly phase of the equatorial QBO in zonal wind and a negative sign in the westerly phase. During the easterly phase, there is more deposition of easterly wave forcing (negative E–P flux divergence anomaly). During the westerly phase, there is less easterly wave forcing, as compared to climatology, so the *anomaly* in E–P flux divergence is positive.

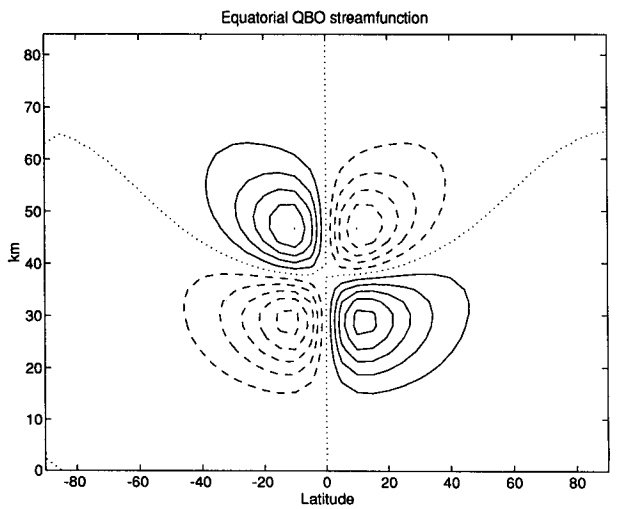


FIG. 3. Equatorial circulation anomaly streamfunction. Contour levels are 0 (dotted line), ±0.005, ±0.01, . . . $m^2 s^{-1}$, with solid (dashed) lines for positive (negative) contours.

It is conceivable that the QBO index for the Southern Hemisphere extratropics is different from that for the Northern Hemisphere extratropics, and that for one year may be different from another within the same hemisphere. This is because the breaking level may be higher if the planetary wave amplitude from the lower atmosphere is lower, and therefore should be affected by the equatorial zonal wind at a higher level. These effects are not incorporated at this stage in our model development.

The *equatorial* column ozone should be correlated with the phase of secondary circulation in the lower stratosphere where most ozone resides, and hence it should be correlated with the zonal wind shear QBO index in that part of the atmosphere (20–30 mb). In the extratropics it is the "downward control" of the circulation induced by breaking above the 10-mb level that produces the QBO anomaly in the column ozone. We should therefore expect to see extratropical column ozone negatively correlated with the equatorial wind at the breaking level, which is higher than what influences column ozone at the equator. For simplicity, however, only a single QBO index is used in the present model. As a compromise it is chosen to be the sign of the 30-mb Singapore wind[1] shifted forward by three months. In Fig. 4, the Singapore wind as a function of time and height is plotted. As can be seen from Fig. 4, the forward shifting in time is equivalent (in most years, 1989 being an exception) to shifting upward by 3 km, as the QBO wind descends at a rate of approximately 1 km $mo^{-1}$. One could alternatively use 10-mb Singapore wind without shifting as an index, with slightly worse effects on the equatorial column ozone, which is affected by the QBO mainly in the 30–20-mb region.

In summary, for the purpose of our model simulation presented in this paper, we specify the seasonal and interannual variations of the E–P flux divergence anomaly $M(\mu, z, t)$ as follows: let $M(\mu, z)$ be given by (2.8), $c(t) = \cos[2\pi t/(12\ \text{mo})]$, and $U(t)$ be the 30-mb Singapore wind; then

$$M(\mu, z, t) = \text{sgn}(U(t + 3\ \text{mo}))[M(\mu, z) - M(-\mu, z) + 2c(t)(M(\mu, z) + M(-\mu, z)) + c(2t)(M(\mu, z) - M(-\mu, z))]/4.$$

This is the simplest annual cycle fit to the four points (two solstice and two equinox points). Note that the power spectrum of $M(\mu, z, t)$ contains peaks at 30, 20, and 8.6 months. Except for the addition of an extra term involving $c(2t)$, it is in the form of $\text{sign}(U)[A + B\sin(2\pi t/12\ \text{mo})]$ discussed in Part I, whose spectrum is plotted in Fig. 7b of Part I.

[1] The variation of the vertical shear of the Singapore wind is in phase with the wind itself.

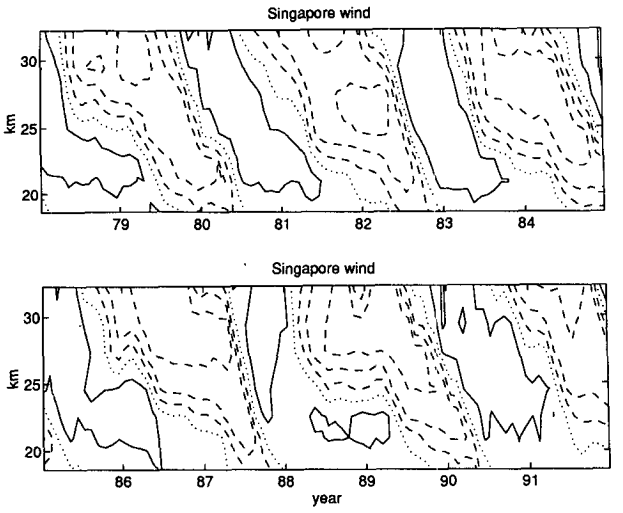


FIG. 4. Singapore wind (Naujokat 1986, with updates) as a function of time and height. Contour levels are 0 (dotted line), ±10, ±20, . . . m $s^{-1}$, with solid (dashed) lines for positive (negative) contours. The vertical coordinate is 7 km × log(1000 mb/pressure).

## 4. Effect of circulation anomaly on column ozone

Since the zonal mean meridional circulation changes are difficult to measure, their existence is often inferred from the tracers transported by the circulation. We will use ozone, in particular, the column density of ozone, for this purpose because global measurements of this quantity are available for comparison.

Let $\bar{\chi}$ be the zonal mean mixing ratio of ozone. The transport of ozone in the meridional plane is described by the following equation (see Tung 1982):

$$\frac{\partial}{\partial t}\bar{\chi} + \frac{\bar{v}(1-\mu^2)^{1/2}}{a}\frac{\partial}{\partial \mu}\bar{\chi} + \bar{w}\frac{\partial}{\partial z}\bar{\chi} - \frac{1}{a^2}\frac{\partial}{\partial \mu}\left(\bar{K}_{yy}(1-\mu^2)\frac{\partial}{\partial \mu}\bar{\chi}\right) = \bar{P} - \bar{L}\bar{\chi}, \quad (4.1)$$

where $\bar{P}$ is the photochemical production, $\bar{L}$ the rate of loss of ozone, and $\bar{K}_{yy}$ is the isentropic mixing coefficient due to the "breaking" of large-scale waves. (Strictly speaking, it is the projection of the isentropic mixing coefficient onto isobaric surfaces that should be used here, but the difference is small, especially when it is the vertically integrated mixing coefficient that is actually used in our simple model.) Irreversible mixing and circulation response to it are interrelated since the E–P flux divergence due to isentropic mixing can be expressed as (see Tung 1986; Yang et al. 1990)

$$F \approx -\bar{K}_{yy}(1-\mu^2)\frac{1}{a}\frac{\partial \bar{q}}{\partial \mu}, \quad (4.2)$$

where $\bar{q}$ is the zonal mean Ertel's potential vorticity. The E–P flux divergence $F$ is in turn related to the circulation through

$$-f\bar{v}(1-\mu^2)^{1/2} \approx F. \tag{4.3}$$

Equation (4.1) can be vertically integrated (after multiplying by $\rho_0$) to yield an evolution equation for column ozone density

$$X \equiv \int_0^\infty \rho_0 \bar{\chi} dz. \tag{4.4}$$

The resulting equation is

$$\frac{\partial}{\partial t} X + \frac{1}{a}\frac{\partial}{\partial \mu}(\langle \bar{v}(1-\mu^2)^{1/2}\rangle X) - \frac{1}{a^2}\frac{\partial}{\partial \mu}\left(\langle \bar{K}_{yy}(1-\mu^2)\rangle \frac{\partial}{\partial \mu} X\right) = S - \langle \bar{L}\rangle X, \tag{4.5}$$

where

$$\langle A\rangle \equiv \int_0^\infty A\rho_0\bar{\chi}dz \Big/ \int_0^\infty \rho_0\bar{\chi}dz \tag{4.6}$$

is the vertical average of $A$ weighted by ozone number density, and

$$S \equiv \int_0^\infty \rho_0 \bar{P} dz \tag{4.7}$$

is the vertically integrated ozone production rate weighted by air density. The only approximation made in deriving (4.5) from (4.1) is

$$\left\langle \frac{\partial}{\partial \mu}(\bar{K}_{yy}(1-\mu^2))\right\rangle \approx \frac{\partial}{\partial \mu}\langle \bar{K}_{yy}(1-\mu^2)\rangle. \tag{4.8}$$

The accuracy of such an approximation has been checked using the 2D quantities in our 2D model and is found to be quite good. Additional approximations on vertical averaging are discussed in the appendix.

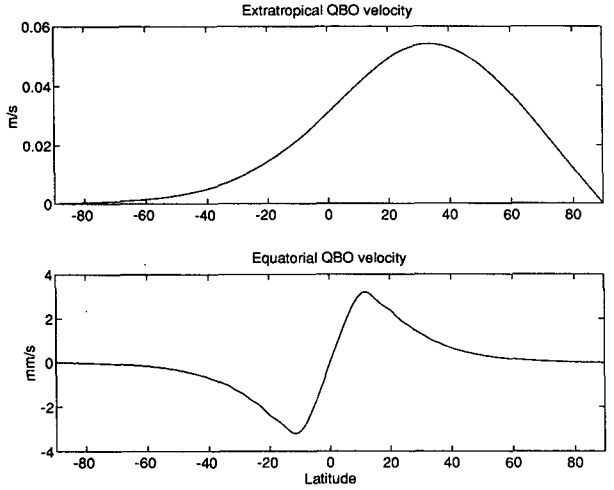


FIG. 5. Ozone-weighted vertically integrated QBO circulation velocity for (a) extratropical circulation and (b) equatorial circulation.

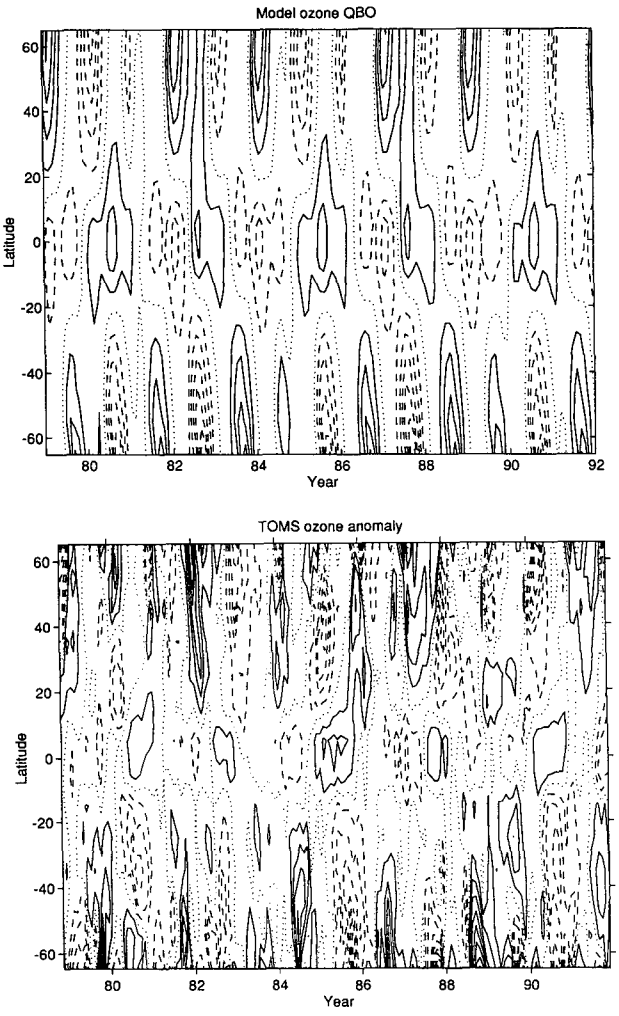


FIG. 6. (a) Model column ozone QBO; (b) TOMS column ozone QBO. Contour levels are 0 (dotted line), ±5 DU, ±10 DU, . . . , with solid (dashed) lines for positive (negative) contours.

The climatological advecting circulation, denoted by $\langle \bar{v}(1-\mu^2)^{1/2}\rangle_0$, and isentropic diffusion coefficient, denoted by $\langle \bar{K}_{yy}(1-\mu^2)\rangle_0$, are shown in the appendix. The anomaly circulation, denoted by $\langle \bar{v}(1-\mu^2)^{1/2}\rangle_1$, is shown here in Fig. 5 for extratropical anomaly (a snapshot during a northern winter in an easterly phase) and for the equatorial QBO circulation (a snapshot during an easterly phase). The two circulations are superimposed to form a global pattern, changing with season and with the phase of the QBO. The anomaly isentropic coefficient consistent with this circulation is calculated using (4.2) and (4.3). These, together with the climatological circulation and climatological diffusion, are used to transport ozone.

## 5. Modeled ozone anomaly

In Fig. 6a, we show our model-produced column ozone anomaly as a function of latitude and time from

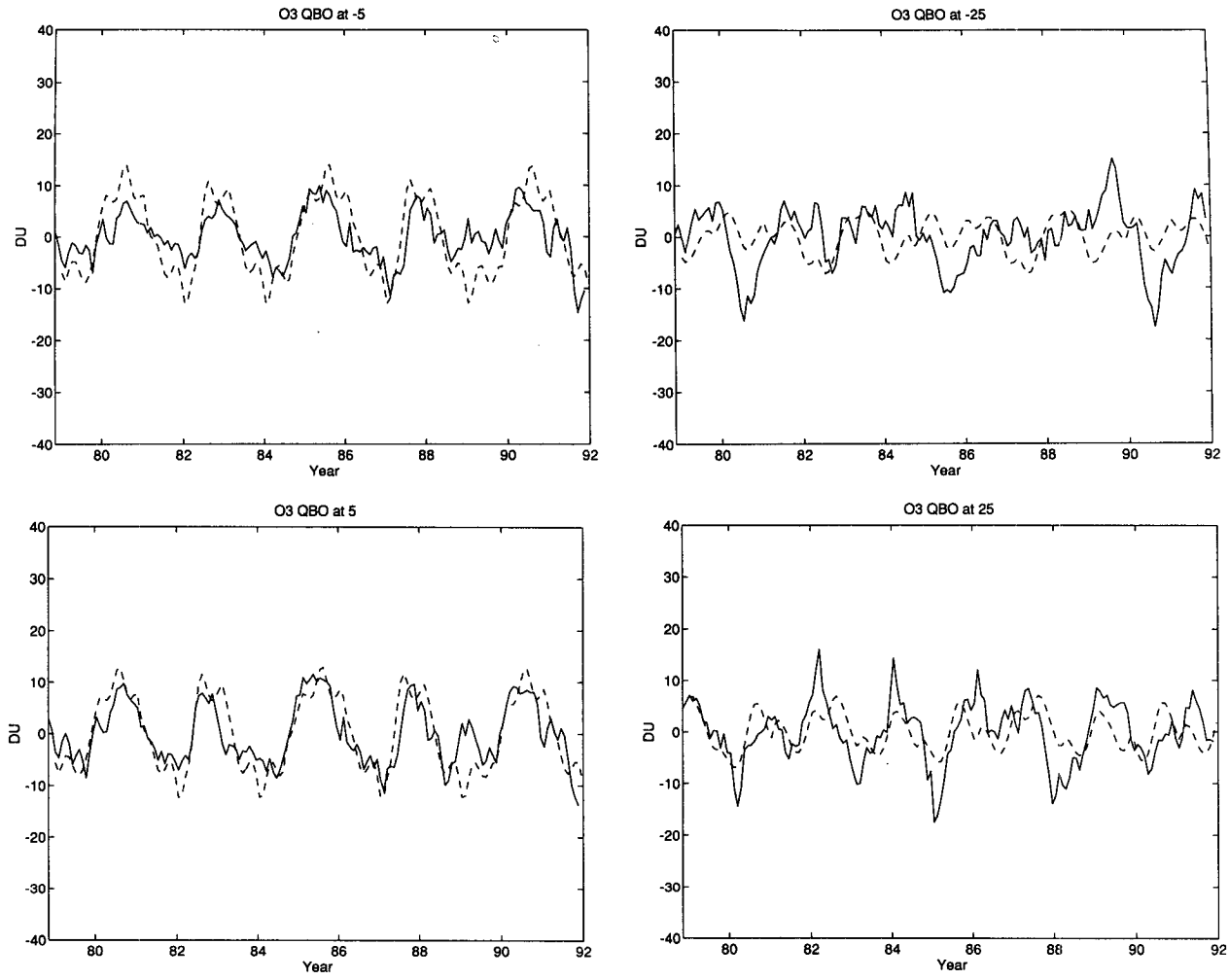


FIG. 7. Comparison of TOMS (solid lines) and model (dashed lines) column ozone QBO at 5, 25, 45, and 65 degrees of latitude in both Northern and Southern Hemispheres.

1979 to 1992. It is to be compared with the TOMS data [version 6, Herman et al. (1991)] shown in Fig. 6b. Figure 6 shows the deseasoned data with an 11-yr solar cycle and the linear trend removed. No filtering to bandpass the QBO frequencies [as was done by Hasebe (1984) and Lait et al. (1989)] has been done. A more detailed comparison of model result with the "unfiltered" data at various latitudes is given in Fig. 7.

In the equatorial region, the modeled and observed ozone agree with each other quite well. This is to be expected because of the good correlation of the observed equatorial column ozone with the observed 30-mb Singapore wind. It has also been successfully modeled previously by Gray and Pyle (1989), Gray and Dunkerton (1990), and Gray and Ruth (1993).

In the subtropics, the amplitude of the modeled QBO is somewhat lower than the observed and weaker than the model result of Gray and Dunkerton (1990) and Holton (1989). This is a result of cancellation in our model between the ozone anomalies generated by tropical and extratropical circulation anomalies, which have opposite sign in the subtropics in our model. However, the modeled phase is correct at ±25°. Both the model and observed ozone anomaly at ±25° are 180° out of phase with the equatorial wind and with the equatorial ozone anomaly.

In the midlatitudes in both hemispheres, the amplitudes (18 DU) of the modeled year to year variation are about the same as the observed. The phases are by and large in agreement, although there are now a few misses: for example, the spring of 1983 in the Southern Hemisphere, and the winters of 1980 and 1989 in the Northern Hemisphere. These are during periods when the QBO winds are in transition (see Fig. 4). The phase of the observed ozone anomaly appears to be negatively correlated with the Singapore wind at a slightly higher level than the level (30 mb) we have adopted as our QBO index.

A striking feature of both the modeled and observed ozone variability at high latitudes (±65°) is the large

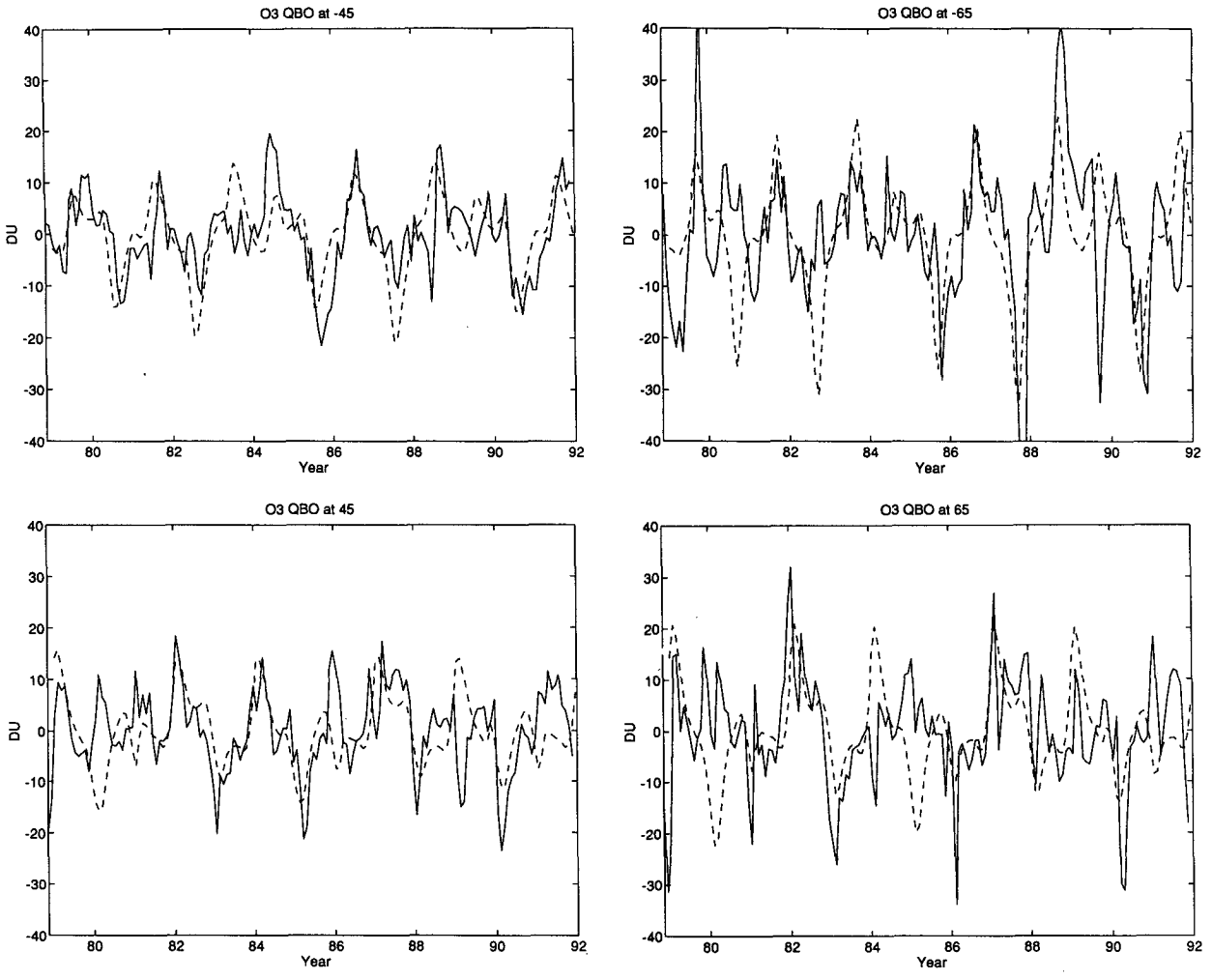


FIG. 7. (*Continued*)

amplitude of interannual variability (20 DU in the Northern Hemisphere and 30 DU in the Southern Hemisphere). These amplitudes would be severely underestimated if the data are filtered to band pass only the frequencies of the equatorial QBO wind. The large peaks in the data now occur in the winter season in the Northern Hemisphere and in the late winter/early spring season in the Southern Hemisphere. This seasonal synchronization, already apparent in the midlatitudes, now becomes the dominant mode of variation in the subpolar latitudes with a frequency centered around 20 months in the model. This is a result of the modulation of the seasonal transport anomaly by the QBO period. This feature is also very prominent in the observed data, as pointed out previously by Schuster et al. (1989) and discussed in detail in Part I. Note that there are also a few misses at high latitudes occurring during the periods of QBO transition in the equatorial wind and/or during the periods when, for some unknown reason, the observed ozone anomaly undergoes another sign change from middle to high latitudes.

In Fig. 8, we compare the spectral density distributions of model results with those of the observations. Please refer to Part I for details of data processing. In the equatorial region, the spectra of both model and observation are dominated by the period of equatorial QBO, peaking near 30 months. The same is true for global ozone. The difference in amplitude between the model and observational results is exaggerated by the fact that the square of the Fourier coefficients is shown.

The 20-month peak emerges in the model in the subtropics and is of about the same amplitude and spectral location as the observation. Note that, as in the observation, the 20-month component has a larger amplitude than the 30-month component in the Northern Hemisphere. The opposite is true in the Southern Hemisphere. This hemispheric difference between the relative amplitudes of the 20-month and 30-month components is well simulated and is due to the hemispheric difference in the model climatological seasonal circulation, which was calculated from the observed temperature. The Brewer–Dobson circulation is stronger

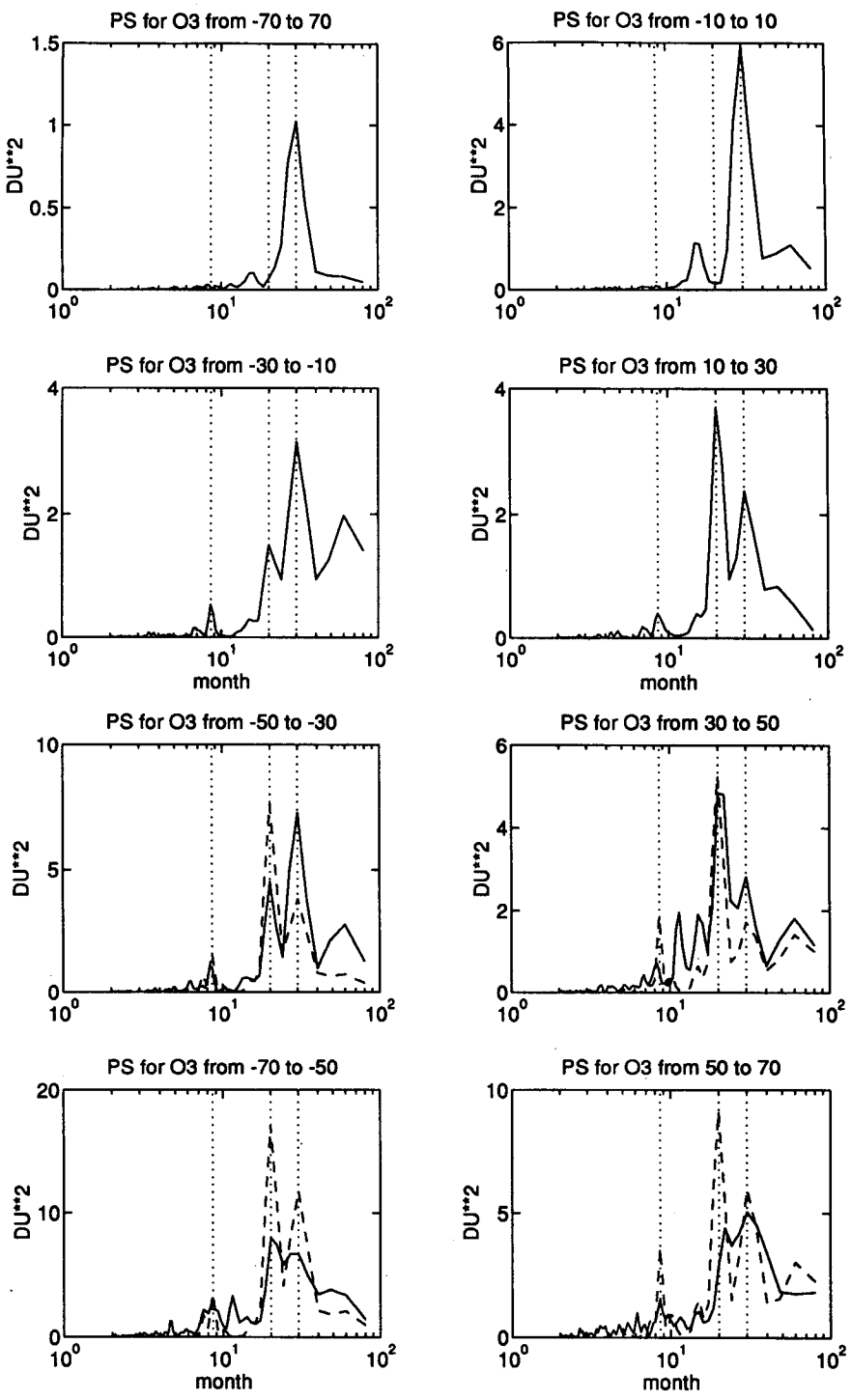


FIG. 8. Power spectrum comparison of TOMS (solid lines) and model (dashed lines) column ozone QBO at various latitude bands. The vertical (dotted) lines mark the positions of 8.6 mo, 20 mo, and 30 mo, respectively.

in the Northern Hemisphere than in the Southern Hemisphere for the same season (see Fig. A1 in the appendix). Interestingly, there is also a good match between the model and data at the 8.6-month period. We have suggested in Part I that these two peaks are result of the difference and the sum of the equatorial QBO frequency 1/(30 mo) and the annual frequency of 1/(12 mo). In our model at least, these are the frequency of

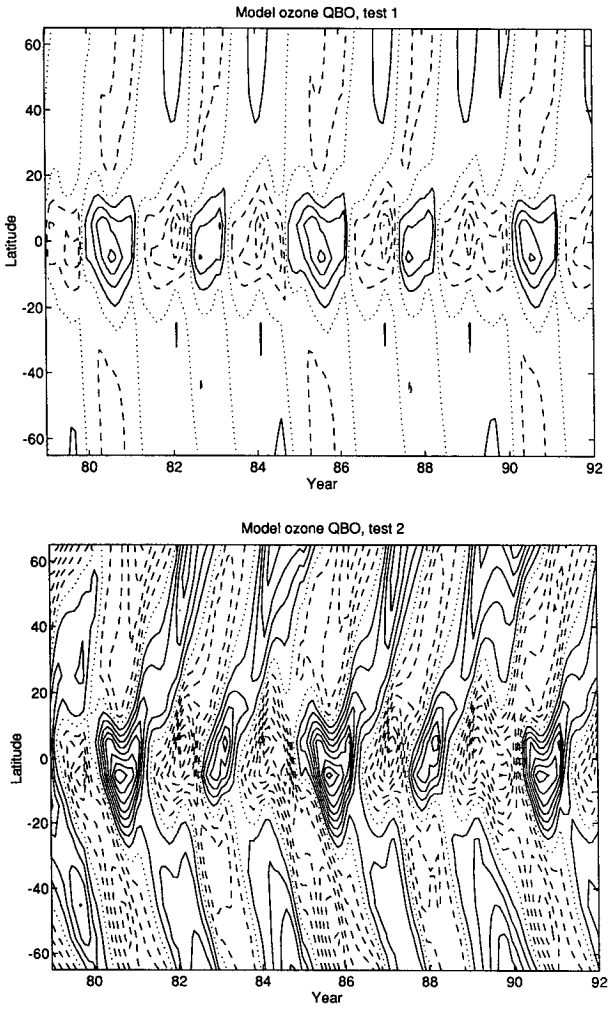


FIG. 9. Model column ozone QBO for two test cases in which extratropical circulation anomaly is surpressed (see text). Contour levels are 0 (dotted line), ±1 DU, ±2 DU, . . . , with solid (dashed) lines for positive (negative) contours.

the extratropical *circulation* anomaly, which arises as the result of tropical QBO modulating a seasonally varying anomaly, as discussed in section 3. This circulation anomaly creates the ozone anomaly in situ. The 30-month anomaly is underestimated by the model in the subtropics, for the reason pointed out earlier.

At middle and high latitudes, both 30- and 20-month peaks are simulated reasonably well. The 20-month component is now more prominent; it is somewhat stronger than the 30-month component in our model results, although for the data the two are comparable. The increase in amplitude of the 20-month peak away from the Tropics suggests that is an anomaly created in situ, not transported from the Tropics.

To investigate the possibility that the QBO anomaly in the extratropics can be caused entirely by transport from the Tropics by the climatological circulation *without* the circulation anomaly in the extratropics, we perform the following two tests. [More tests can be found in Tung and Yang (1993).] In the first test, the circulation anomaly in the extratropics driven by E−P flux divergence anomaly described in section 3 is switched off; only the tropical QBO forcing and the background (climatological) circulation are present. The amplitude of the tropical wave forcing is the same as that in Gray and Pyle (1989) and is also the same as that adopted in the previous section. The result is shown in Fig. 9a. At middle and high latitudes, the model ozone anomaly has decreased to about 1 DU, compared to the observed 20–30 DU. This is because the chemical and dynamical dampings reduce the QBO anomaly as it is being transported from the Tropics. In the second test, both chemical and dynamical damping are reduced by a factor of 5. The model ozone anomaly (shown in Fig. 9b) now has an amplitude of about 3–4 DU at middle and high latitudes, still much smaller than the observed.

The power spectra of the results of these two tests at selected latitude bands are shown in Fig. 10. Note that the model ozone anomaly with tropical forcing has essentially only one peak at the 30-month period with much reduced amplitude in its spectrum. The 20-month and the 8.6-month peaks are almost entirely missing. Increasing tropical QBO forcing will not change this. Therefore, based on these test results, we conclude that the existence of an extratropical circulation anomaly is not only consistent with the spectral signature of the observed ozone QBO, but is also *necessary* to explain it.

## 6. Conclusions and discussion

Our modeling work suggests that the interannual variability in column ozone in the extratropics attributable to QBO has so far been underestimated. It appears that the bulk of column ozone's interannual variability in the "unfiltered" data can be accounted for by the extratropical QBO mechanism proposed here (our model has only the seasonal cycle and the equatorial QBO phase, and no other forms of interannual variability). It involves the indirect effect of the equatorial QBO modulation of the seasonal cycle of the extratropical circulation anomaly, resulting in a shift in period of variability from the QBO period (30 mo during the last decay) in the Tropics to 20 months in the high latitudes where the seasonal cycle is strong (see Part I). The maximum amplitude of the anomaly occurs during winter in the Northern Hemisphere and late winter and early spring in the Southern Hemisphere. This seasonal synchronization has been pointed out previously by many authors (e.g., Hamilton 1989; Holton 1989; Gray and Dunkerton 1990).

We suggest that it is almost impossible to simulate both the phase and the amplitude of the unfiltered ozone anomaly in the extratropics by the mechanism of transport of equatorial QBO anomaly to high latitudes. Such a mechanism can account for no more than one-tenth of the observed amplitude and would have produced an incorrect phase when compared to the unfiltered data.

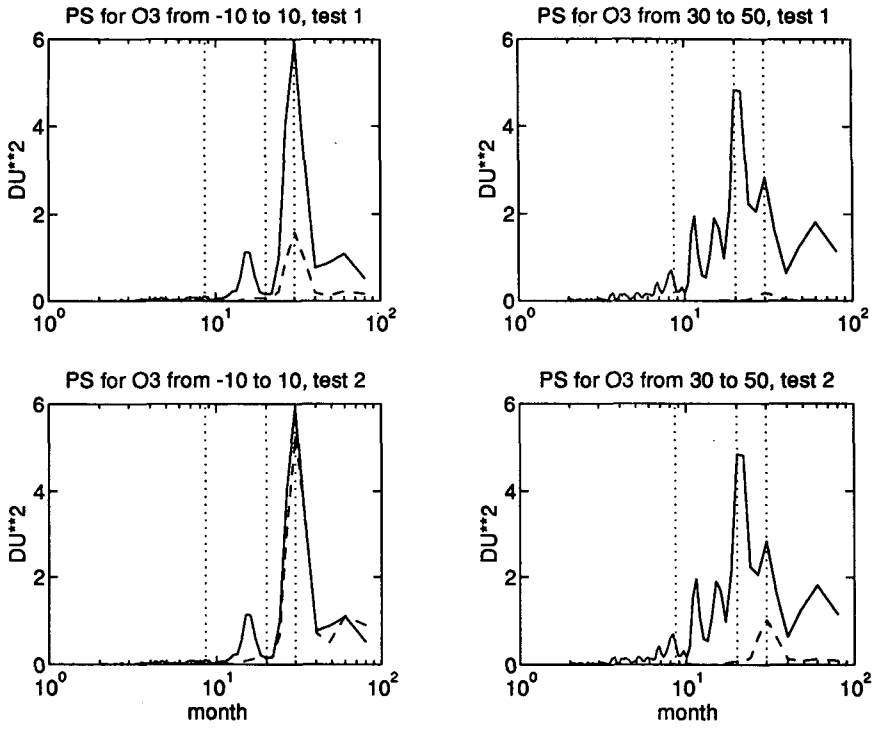


FIG. 10. Power spectrum comparison of TOMS (solid lines) and model (dashed lines) column ozone QBO at selected latitude bands for the two test cases shown in Fig. 9. The vertical (dotted) lines mark the positions of 8.6, 20, and 30 months, respectively.

We further suggest that the extratropical QBO anomaly in column ozone is a manifestation of the extratropical QBO anomaly in the transporting circulation. Negative (positive) column ozone anomaly is created in situ by upward (downward) circulation in the lower stratosphere. There is no need for such an (ozone) anomaly to be transported to the higher latitudes from the equatorial region.

In this very simple model, the QBO modulation of the planetary wave breaking process is hypothesized instead of modeled. However, other authors have modeled this process with some success. O'Sullivan and Salby (1990) performed a high-resolution numerical simulation of the planetary wave breaking process using their equivalent barotropic model. They found a higher tendency for the planetary waves to break in the presence of an easterly momentum source in the Tropics. Recently, O'Sullivan and Young (1992) found, using a mechanistic 3D primitive equation model, that the polar vortex is more (less) disturbed in the easterly (westerly) phase of the QBO and suggested the importance of nonlinear critical layers. Holton and Austin (1991) found that their three-dimensional numerical model tends to produce stratospheric sudden warmings, an extreme manifestation of breaking events, during the easterly phase of the equatorial QBO for moderate planetary wave forcings. Similar numerical tests have also been performed by Dameris and Ebel (1990) and Kodera et al. (1991). The recently proposed parameterization of planetary wave breaking by Garcia (1991) provides a plausible explanation for the enhanced tendency of breaking in the easterly phase. (The criterion $q_y = \bar{q}_y + q'_y < 0$ tends to be satisfied more poleward and at a lower level when $|q'_y|$ is larger.)

The present model is not prognostic because the phase of the equatorial zonal wind QBO is specified. Recently Wallace et al. (1993) discussed an intriguing and simple prediction scheme for the phase progression of equatorial QBO wind that is more accurate relative to a model that treats the QBO as a purely periodic phenomenon. It will be interesting to introduce this and other prognostic schemes into our model to test the feasibility of predicting both tropical and extratropical QBO a few years in advance.

*Acknowledgments.* This research is supported by NSF Grant ATM-8903340 and by NASA Grants NAGW-1605 and NAG-1-1404.

## APPENDIX

### Model for Column Ozone, Model Parameters

The vertical weighting function in (4.5) and (4.6) involves the total ozone vertical profile, which consists of the climatological profile and the QBO profile. The latter is part of the solution to Eq. (4.1) and should be treated as an unknown. Fortunately, the total ozone profile differs only slightly from the climatological profile

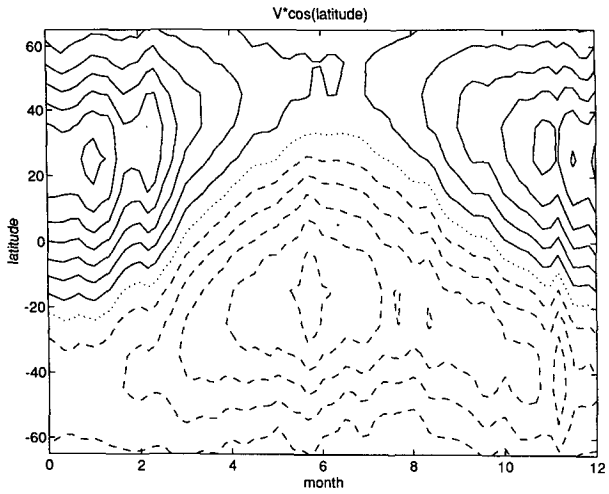


FIG. A1. Meridional velocity $\langle \bar{v} \cos\varphi \rangle_0$. Contour levels are 0 (dotted line), $\pm 3$, $\pm 6$, ... km day$^{-1}$, with solid (dashed) lines for positive (negative) contours.

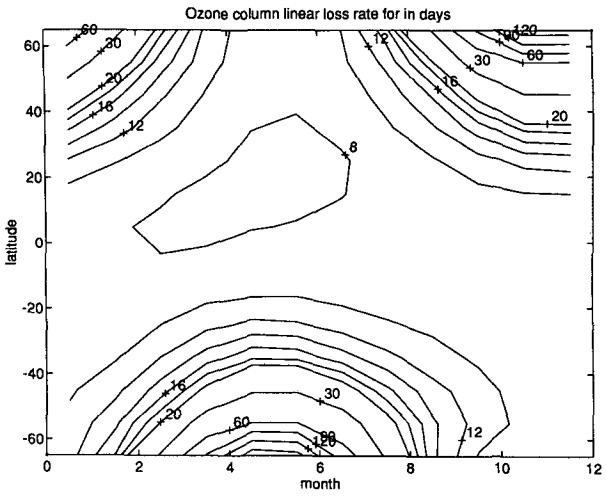


FIG. A3. Ozone column linear loss time $1/L_0$ as defined in Eq. (A.2).

and can, in some cases, be approximated by the climatological vertical profile of ozone. Our tests show that for quantities such as $\bar{v}$ and $K_{yy}$, which have broad features vertically, this is a good approximation. It also does not matter significantly whether latitudinal variation of the climatological ozone profile is taken into account. The ozone loss rate $L$, on the other hand, varies rather rapidly with height, and so $\langle \bar{L} \rangle$ cannot be adequately approximated by the integral of $L$ weighted with climatological ozone. The part due to anomaly ozone weighting is included in this study, as discussed later.

We have calculated the climatological meridional velocity $\langle \bar{v}(1 - \mu^2)^{1/2} \rangle_0$ and the isentropic mixing coefficient $\langle \bar{K}_{yy}(1 - \mu^2)^{1/2} \rangle_0$ using the observed NMC zonal mean temperature for the 10-yr period 1979–1988. Climatological values (i.e., without QBO variation) are denoted by subscript zero. The procedure has been described in Yang et al. (1990). It uses our 2D model [Yang et al. (1991)] and a comprehensive radiative transfer code [Olaguer et al. (1992)]. The climatology is the average of the individual year results. Figure A1 for $\langle \bar{v}(1 - \mu^2)^{1/2} \rangle_0$ generally shows poleward transport in both hemispheres for all seasons. The climatological isentropic mixing coefficient consistent with the circulation in Fig. A1 is shown in Fig. A2.

The ozone loss rate was calculated using our 2D model with full chemistry; the climatological loss time $1/L_0$ is shown in Fig. A3. As expected it shows at high latitudes shorter photochemical damping time in the summer season of the respective hemisphere (of about 10 days) than the winter season (about 2 to 3 months).

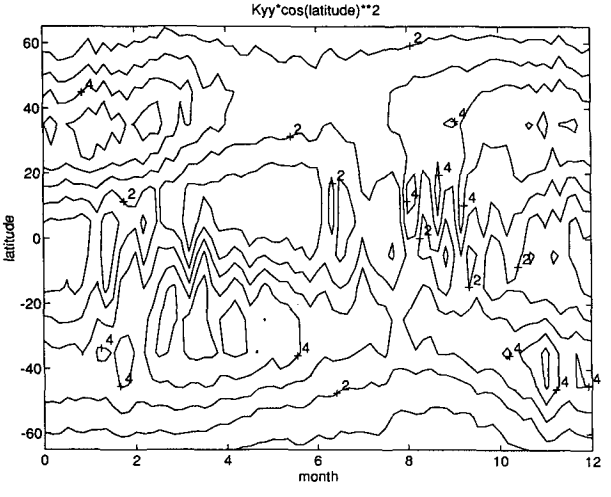


FIG. A2. Isentropic mixing coefficient $\langle \bar{K}_{yy} \cos^2\varphi \rangle_0$. Contour interval is $10^9$ cm$^2$ s$^{-1}$.

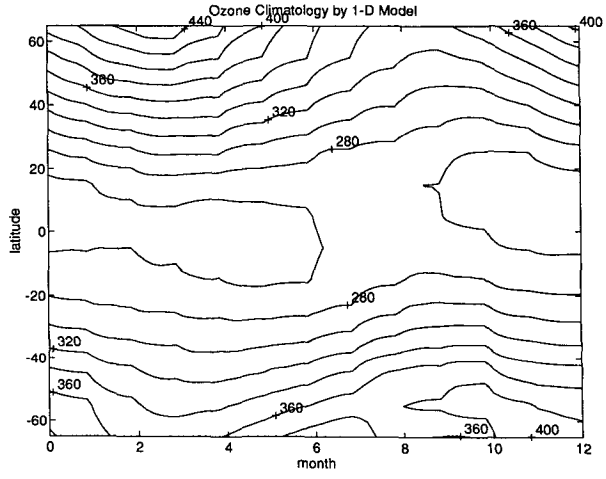


FIG. A4. Model column ozone climatology in DU.

In the Tropics, the chemical loss time is about 10 days for all seasons.

With the climatological transport and chemical production and loss rates imported from our 2D model, the climatological column ozone $X_0$ can readily be generated by solving the simple one-dimensional equation (4.5). The result is shown in Fig. A4. The observed TOMS climatology for the period 1979–1991 is shown in Fig. A5. The model result is found to be satisfactory, as was found previously with our original 2D model (see Yang et al. 1991).

A correct simulation of ozone climatology is necessary for our later simulation of ozone QBO anomaly, because part of the anomaly is caused by the anomalous transport of the climatology.

Unlike the other quantities, $1/\langle\bar{L}\rangle$ is sensitively dependent on the choice of weighting functions. This is because $1/L$ varies rapidly with height, ranging from a few tens of days to a few hundred days between 30 and 20 km [see Fig. 6 of Gray and Pyle (1989)]. The loss timescale shown in Fig. A3 is appropriate for climatological ozone, but is probably too short for the QBO ozone anomaly. No significant ozone QBO can be generated by our model using these short timescales even when the QBO component of the transport parameters is increased by a factor of ten.

To emphasize the different weighting functions for climatology and anomaly, we rewrite $\langle\bar{L}\rangle X$ as

$$\int_0^\infty \bar{L}\rho_0\bar{\chi}dz = \int_0^\infty \bar{L}\rho_0\bar{\chi}_0dz + \int_0^\infty \bar{L}\rho_0\bar{\chi}_1dz = L_0X_0 + L_1X_1, \quad \text{(A.1)}$$

where we use the subscript 0 to denote climatology and the subscript 1 to denote the deviation from climatology (the QBO component in the present model). It is then seen that two different loss rates emerge:

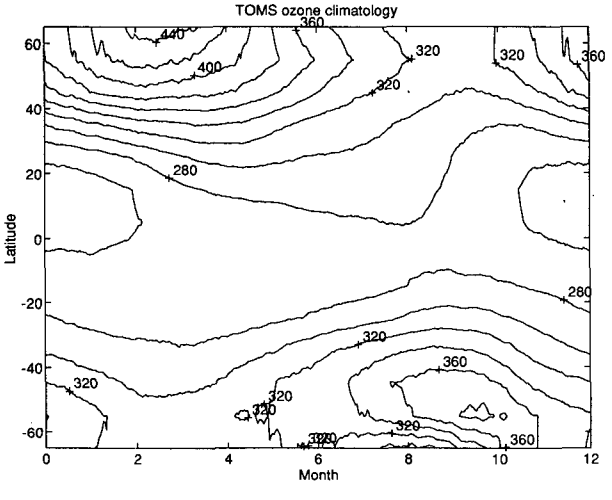


FIG. A5. TOMS column ozone climatology in DU.

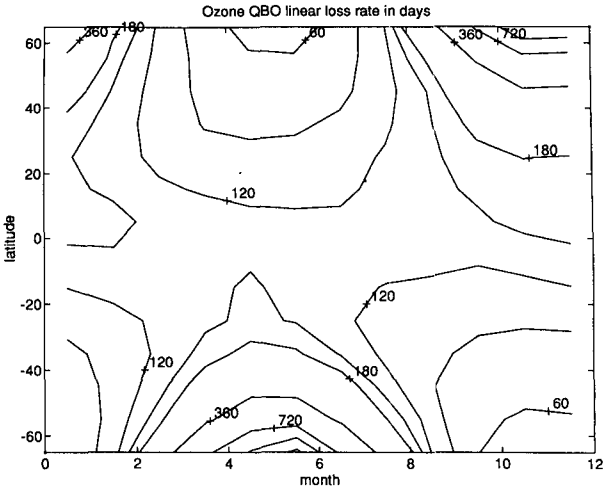


FIG. A6. Ozone QBO linear loss time $1/L_1$ as defined in Eq. (A.3).

$$L_0 \equiv \int_0^\infty \bar{L}\rho_0\bar{\chi}_0dz \Big/ \int_0^\infty \rho_0\bar{\chi}_0dz \quad \text{(A.2)}$$

is the loss rate weighted by the climatological profile $\bar{\chi}_0$, and

$$L_1 \equiv \int_0^\infty \bar{L}\rho_0\chi_1dz \Big/ \int_0^\infty \rho_0\bar{\chi}_1dz \quad \text{(A.3)}$$

is the loss rate weighted by the QBO anomaly. The first is the appropriate rate for the climatological column ozone, while the second is the appropriate one for the QBO anomaly in column ozone. No approximation is made in (A.1). The second term on the right-hand side of (A.1), $L_1X_1$, is small compared with the first term $L_0X_0$, but it should be retained since we are interested in ozone anomaly here. When climatology is subtracted from Eq. (4.5), $L_0X_0$ is absent and $L_1X_1$ is the only chemical term remaining in the resulting equation for ozone QBO anomaly.

Observed vertical profile (e.g., see Zawodny and McCormick 1991) shows that the dynamical QBO component is mostly in the region between 20 and 30 km, and in this altitude range the vertical variation of anomaly ozone number density is dominated by the variation of air density. We therefore evaluate $L_1$ approximately as

$$L_1 \sim \int_{20\text{ km}}^{30\text{ km}} \bar{L}\rho_0dz \Big/ \int_{20\text{ km}}^{30\text{ km}} \rho_0dz. \quad \text{(A.4)}$$

The result is plotted in Fig. A6. The weighted average is dominated by the lower loss rates appropriate for the dynamical region of the lower stratosphere. The chemical damping time is about 5 months in the Tropics (vs less than 2 weeks for $L_0$ in Fig. A3). The variation in middle and high latitudes is very dependent on season but independent of hemisphere. The chemical damping time goes through a simple (but strong) annual varia-

tion with long timescales in winter and short timescales in summer.

## REFERENCES


Chipperfield, M. P., and L. J. Gray, 1992: Two-dimensional model studies of the interannual variability of trace gases in the middle atmosphere. *J. Geophys. Res.*, **97,** 5963–5980.

Dameris, M., and A. Ebel, 1990: The quasi-biennial oscillation and major stratospheric warmings: A three-dimensional model study. *Ann. Geophys.*, **8,** 79–86.

Dunkerton, T. J., and M. P. Baldwin, 1991: Quasi-biennial modulation of planetary-wave fluxes in the Northern Hemisphere winter. *J. Atmos. Sci.*, **48,** 1043–1061.

——, D. P. Delisi, and M. P. Baldwin, 1988: Distribution of major stratospheric warmings in relation to the quasi-biennial oscillation. *Geophys. Res. Lett.*, **15,** 136–139.

Garcia, R. R., 1987: On the mean meridional circulation of the middle atmosphere. *J. Atmos. Sci.*, **44,** 3599–3609.

——, 1991: Parameterization of planetary wave breaking in the middle atmosphere. *J. Atmos. Sci.*, **48,** 1405–1419.

Gray, L. J., and J. A. Pyle, 1989: A two dimensional model of the quasi-biennial oscillation of ozone. *J. Atmos. Sci.*, **46,** 203–220.

——, and T. J. Dunkerton, 1990: The role of the seasonal cycle in the quasi-biennial oscillation of ozone. *J. Atmos. Sci.*, **47,** 2429–2451.

——, and S. Ruth, 1993: The modeled latitudinal distribution of ozone quasi-biennial oscillation using observed equatorial winds. *J. Atmos. Sci.*, **50,** 1033–1046.

Hamilton, K., 1989: Interhemispheric asymmetry and annual synchronization of the ozone quasi-biennial oscillation. *J. Atmos. Sci.*, **46,** 1019–1025.

Hasebe, F., 1984: The global structure of the total ozone fluctuations observed on the time scales of two to several years. *Dynamics of the Middle Atmosphere,* J. R. Holton and T. Matsuno, Eds., D. Reidel, 445–464.

Herman, J. R., R. Hudson, R. McPeters, R. Stolarski, Z. Ahmad, X.-Y. Gu, S. Taylor, and C. Wellemeyer, 1991: A new self-calibration method applied to TOMS and SBUV backscattered ultraviolet data to determine long-term global ozone change. *J. Geophys. Res.*, **96,** 7531–7545.

Holton, J. R., 1989: Influence of the annual cycle in meridional transport on the quasi-biennial oscillation in total ozone. *J. Atmos. Sci.*, **46,** 1434–1439.

——, and H. C. Tan, 1980: The influence of the equatorial quasi-biennial oscillation on the global circulation at 50 mb. *J. Atmos. Sci.*, **37,** 2200–2208.

——, and ——, 1982: The quasi-biennial oscillation in the Northern Hemisphere lower stratosphere. *J. Meteor. Soc. Japan,* **60,** 140–148.

——, and J. Austin, 1991: The influence of the equatorial QBO on sudden stratospheric warmings. *J. Atmos. Sci.*, **48,** 607–618.

Kodera, K., M. Chiba, and K. Shibata, 1991: A general circulation model study of the solar and QBO modulation of the stratospheric circulation during the Northern winter. *Geophys. Res. Lett.*, **18,** 1209–1212.

Labitzke, K., 1982: On the interannual variability of the middle stratosphere during the Northern winters. *J. Meteor. Soc. Japan,* **67,** 29–41.

Lait, L. R., M. R. Schoeberl, and P. A. Newman, 1989: Quasi-biennial modulation of the Antarctic ozone depletion. *J. Geophys. Res.*, **94,** 550–571.

Leovy, C. B., C.-R. Sun, M. H. Hitchman, E. E. Remsberg, J. M. Russel III, L. L. Gordley, J. C. Gille, and L. V. Lyjak, 1985: Transport of ozone in the middle stratosphere: Evidence for planetary wave breaking. *J. Atmos. Sci.*, **42,** 230–244.

McIntyre, M. E., 1982: How well do we understand the dynamics of stratospheric warmings? *J. Meteor. Soc. Japan,* **60,** 37–65.

——, and T. N. Palmer, 1984: The 'surf zone' in the stratosphere. *J. Atmos. Terr. Phys.*, **46,** 825–849.

Naujokat, B., 1986: An update of the observed quasi-biennial oscillation of the stratospheric winds over the tropics. *J. Atmos. Sci.*, **43,** 1873–1877.

Olaguer, E. P., H. Yang, and K. K. Tung, 1992: A reexamination of the radiative balance of the stratosphere. *J. Atmos. Sci.*, **49,** 1242–1263.

O'Sullivan, D., and M. L. Salby, 1990: Coupling of the quasi-biennial oscillation and the extratropical circulation in the stratosphere through planetary wave transport. *J. Atmos. Sci.*, **47,** 650–673.

——, and R. E. Young, 1992: Modeling the quasi-biennial oscillation's effect on the winter stratospheric circulation. *J. Atmos. Sci.*, **49,** 2437–2448.

Pawson, S., K. Labitzke, B. Naujokat, R.-S. Wang, and K. Graedrich, 1993: Intraseasonal tropical–extratropical interactions observed in the stratosphere. *Coupling Processes in the Lower and Middle Atmosphere,* E. V. Thrane, T. A. Blix, and D. C. Fritts, Eds., Kluwer Academic, 35–47.

Plumb, R. A., 1982: Zonally symmetric Hough modes and meridional circulations in the middle atmosphere. *J. Atmos. Sci.*, **39,** 983–991.

——, 1984: The quasi-biennial oscillation. *Dynamics of the Middle Atmosphere,* J. R. Holton and T. Matsuno, Eds., D. Reidel, 217–251.

——, and R. C. Bell, 1982: A model of the quasi-biennial oscillation on an equatorial beta-plane. *Quart. J. Roy. Meteor. Soc.*, **108,** 335–352.

Randel, W. J., 1993: Global variations of zonal-mean ozone during stratospheric warming events. *J. Atmos. Sci.*, **50,** 3308–3321.

Schuster, G., R. Rood, and M. Schoeberl, 1989: Quasi-biennial and interannual variability in high resolution total ozone data (TOMS). *Ozone in the Atmosphere,* Göttingen, R. D. Bojkov and P. Fabian, Eds., Deepak, 260–264.

Tung, K. K., 1982: On the two-dimensional transport of stratospheric trace gases in isentropic coordinates. *J. Atmos. Sci.*, **39,** 2330–2355.

——, 1986: Nongeostrophic theory of zonally averaged circulation. Part I: Formulation. *J. Atmos. Sci.*, **43,** 2600–2618.

——, and H. Yang, 1993: On global quasi-biennial oscillation in column ozone. *Coupling Processes in Middle and Lower Atmospheres,* E. V. Thrane, T. A. Blix, and D. C. Fritts, Eds., Kluwer Academic, 1–24.

Wallace, J. M., R. L. Panetta, and J. Estberg, 1993: Representation of the equatorial stratospheric quasi-biennial oscillation in EOF phase space. *J. Atmos. Sci.*, **50,** 1751–1762.

Yang, H., K. K. Tung, and E. P. Olaguer, 1990: Nongeostrophic theory of zonally averaged circulation. Part II: Eliassen–Palm flux divergence and isentropic mixing coefficient. *J. Atmos. Sci.*, **47,** 215–241.

——, E. Olaguer, and K. K. Tung, 1991: Simulation of the present-day atmospheric ozone, odd nitrogen, chlorine and other species using a coupled 2D model in isentropic coordinates. *J. Atmos. Sci.*, **48,** 442–471.

Zawodny, J. M., and M. P. McCormick, 1991: Stratospheric Aerosol and Gas Experiment II measurements of the quasi-biennial oscillations in ozone and nitrogen dioxide. *J. Geophys. Res.*, **96,** 9371–9377.